NASA Technical Paper 1654

Realizable Optimal Control for a Remotely Piloted Research Vehicle

H. J. Dunn

MAY 1980

NASA

NASA Technical Paper 1654

Realizable Optimal Control for a Remotely Piloted Research Vehicle

H. J. Dunn
Langley Research Center
Hampton, Virginia

National Aeronautics
and Space Administration

**Scientific and Technical
Information Office**

1980

SUMMARY

This paper describes the design of a control system using linear-quadratic-regulator (LQR) control law theory for time invariant systems in conjunction with an "incremental gradient" procedure. The incremental gradient technique is used to reduce the full-state feedback controller design, generated by the LQR algorithm, to a realizable controller design. With a realizable controller, the feedback gains are based only on the available system outputs instead of being based on the full-state outputs as with the LQR approach. The controller design is for a remotely piloted research vehicle (RPRV) stability augmentation system. Included in the design are methods for accounting for noisy measurements, discrete controls with zero-order-hold (ZOH) outputs, and computational delay errors. Results from simulation studies of the response of the RPRV to a step in the elevator and frequency analysis techniques are included to illustrate the abnormalities and their influence on the final controller design.

INTRODUCTION

This paper describes the use of linear-quadratic regulator (LQR) theory for time invariant systems to design a stability augmentation system (SAS) for a remotely piloted research vehicle (RPRV). Classical control theory based designs for this aircraft have had marginal results, partly because of the design problem having multiple inputs and partly because of the controller having to be implemented with a digital computer. This paper designs a SAS for an RPRV with a design methodology that accounts for noisy measurements, discrete controls with zero-order-hold (ZOH) outputs, and computational delay errors.

There has been considerable attention in the past to the use of LQR theory for the design of control systems. (See refs. 1 to 3.) In general, these designs require the full state to be measured or reconstructed from the available outputs and used in the control system. Although it may be theoretically possible to obtain the full state, more often than not, as the complexity of the problem increases, the ability to obtain the full state becomes impossible; for example, the active control flutter models are of the order of 100 states.

Recently, there has been a methodology developed (ref. 4) that retains the generality of quadratic optimization while resulting in a control system that is realizable. The term realizable is used here to mean a control system that employs feedback gains only on the available outputs, instead of being based on the full state as with the LQR approach.

The design process is divided into two stages. The first step is identical with the LQR procedure. The designer, in an iterative process, adjusts the cost functions until the desired closed-loop control system response is obtained. Once this objective is achieved, the design is reduced to a realizable form with the use of an "incremental gradient" procedure. This procedure can be regarded as a two-point boundary-value problem in the gain state space, the initial

conditions being the LQR algorithm gains and the terminal conditions being the desired controller configuration, that is, with gains on inaccessible states equal to zero.

SYMBOLS

A	system matrix
$\tilde{A}$	defined in equation (A10)
A_1, A_2	dummy variable
a_z	sensor output, normal acceleration, g
A_{RB}	rigid-body system matrix (eq. (4))
B	control input matrix (eq. (5))
D	control response matrix
E	statistical expectation
$\tilde{E}$	defined in equation (A11)
G_1	control input matrix
G_2	disturbance input matrix
H	state response matrix
$J, \bar{J}$	quadratic performance indices
$j = \sqrt{-1}$	
K	state optimal feedback gain matrix
$K^*(\lambda)$	defined by equation (A18)
$K_1(\lambda)$	gains on selected measurements
K_2	gains on eliminated measurements
M	measurement matrix
P	Lagrange multipliers
Q	symmetric weighting matrix
$\tilde{Q}$	defined in equation (A12)
q	aircraft pitch rate, rad/sec

q_s sensor output, q, rad/sec

R control weighting matrix

R_1 response covariance matrix

r_1 design response vector

$\bar{r}_1$ augmented design response vector

r_2 measurement response vector

$\text{rms}(x) = \left\{E\left[(x - E(x))^2\right]\right\}^{1/2}$

s Laplace transform

t time, sec

tr matrix trace

u control input vector (eq. (2))

v aircraft perturbation from steady-state velocity, m/s

v_s sensor output, v, m/s

X state covariance matrix

x_{RB} rigid body state vector (eq. (4))

x system state vector

x_g gust state

Z z transform

α aircraft perturbation in angle of attack, rad

α_s sensor output, angle of attack, rad

δ_c canard position, rad

$\delta_{c,c}$ canard command, rad

δ_e elevator position, positive for trailing edge down, rad

$\delta_{e,c}$ elevator command, rad

δ_{fi} inboard flap position, rad

$\delta_{fi,c}$ inboard flap command, rad

δ_{fo} outboard flap position, rad

$\delta_{fo,c}$ outboard flap command, rad

η unit variance white noise vector

η_1, η_2 elements of vector

θ aircraft perturbation in pitch angle, rad

θ_s sensor output, θ, rad

ρ scalar design parameter

σ real part of eigenvalue

τ time constant

ϕ phase angle, deg

ω frequency of input signal

ω_s sampling frequency, rad/sec

Dots over symbols denote derivatives with respect to time.

A primed symbol denotes a transpose.

PROBLEM STATEMENT

The problem considered in this report consists of the design of a stability augmentation system (SAS) for a 0.44-scale model of an advanced fighter remotely piloted research vehicle (RPRV). The RPRV is launched from the wing of a B-52 airplane, controlled from the ground station by a digital computer, and backed up by a chase airplane which is capable of safely returning the RPRV to base. This advanced fighter configuration has 10 independently controlled aerodynamic surfaces which are grouped into 5 longitudinal controls (that is, controls that produce motions in the vertical plane of the aircraft) and 5 lateral controls (that is, horizontal-motion-producing controls). Because of its aerodynamic design, the vehicle is longitudinally unstable for a large part of its subsonic flight envelope. The purpose of this paper is to design a SAS that will stabilize the RPRV longitudinally and provide adequate flying characteristics. Since the design methodology is the same for each flight condition, only the longitudinal equation of motion for one flight condition is presented. The control must be implemented on a ground computer with sensor information being received and control commands being transmitted at a rate of 50 Hz. This sampling rate is fixed for the problem and is not considered a design variable. The time required to receive the data, to calculate the command, and to transmit the command to the RPRV is approximately the time of 1 cycle; thus, a 1-cycle delay (20 ms) is assumed between receiving the sensor signal and transmitting the control command. For the design model, sensors were assumed

to have sufficient bandwidth to permit them to be modeled with a unity transfer function. Sensor noise was modeled by shaping white noise through a first-order low-pass filter. Estimated sensor noise parameters, based on aircraft flight records (ref. 5), are given in table I. The use of sensor noise characteristics based on flight data was deemed more appropriate since it includes the effects of instrument noise, aeroelastic effects, turbulence effects, engine vibration, etc., and would represent the worst-case situation.

The design of the SAS for the entire flight envelope requires that the nonlinear equations of motion be linearized about several flight conditions, the design process applied at each of the conditions, and some procedure be defined for changing the control system parameters as a function of the flight condition.

The linearized equations of motion in the longitudinal plane for the rigid body states of the RPRV in level flight at an altitude of 30 480 km (10 000 ft) and a Mach number of 0.9 are

$$\frac{d}{dt}\begin{bmatrix} v \\ \alpha \\ q \\ \theta \end{bmatrix} = \begin{bmatrix} -0.0451 & -67.62 & -74.31 & -105.4 \\ 0 & -2.498 & 0.987 & -0.0008 \\ -0.0060 & 72.41 & -3.803 & 0.0012 \\ 0 & 0 & 1. & 0 \end{bmatrix} \begin{bmatrix} v \\ \alpha \\ q \\ \theta \end{bmatrix} + \begin{bmatrix} 7.579 & -4.859 & 0.2274 & -0.8891 \\ -0.3469 & -0.1864 & 0.0092 & -0.0341 \\ -85.36 & -49.03 & 17.11 & -11.80 \\ 0 & 0 & 0 & 0 \end{bmatrix} \begin{bmatrix} \delta_e \\ \delta_{fi} \\ \delta_c \\ \delta_{fo} \end{bmatrix} \tag{1}$$

where v is the perturbation from the steady-state velocity in meters per second; α is the perturbation in angle of attack in radians; q is the pitch rate in radians per second; θ is the perturbation in pitch angle in radians; δ_e, δ_{fi}, δ_c, and δ_{fo} are the elevator, inboard flap, canard, and outboard flap position in radians. The fifth longitudinal command, the speed brake, was omitted because of its ineffectiveness, as compared with the other controls. The open-loop pole locations are shown in figure 1. The control actuators are represented by first-order 40-radian actuators with unity static gain. By combining the rigid-body states with the actuator states, the basic RPRV equations of motion can be written as

$$\dot{x} = Ax + G_1 u \tag{2}$$

$$r_2 = Mx \tag{3}$$

In these equations, x is the system state vector with the following definitions:

$$x = \begin{bmatrix} v \\ \alpha \\ q \\ \theta \\ \delta_e \\ \delta_{fi} \\ \delta_c \\ \delta_{fo} \end{bmatrix}$$

Velocity, m/s
Angle of attack, rad
Pitch rate, rad/sec
Pitch angle, rad
Actuator position, rad
Actuator position, rad
Actuator position, rad
Actuator position, rad

u is the control input vector with the following definitions:

$$u = \begin{bmatrix} \delta_{e,c} \\ \delta_{fi,c} \\ \delta_{c,c} \\ \delta_{fo,c} \end{bmatrix}$$

Elevator command, rad
Flaps-inboard command, rad
Canard command, rad
Flaps-outboard command, rad

and r_2 is the measurement response vector with the following definitions:

$$r_2 = \begin{bmatrix} v_s \\ \alpha_s \\ q_s \\ \theta_s \\ a_z \\ \delta_{fi} \\ \delta_c \\ \delta_{fo} \end{bmatrix}$$

Velocity, m/s
Angle of attack, rad
Pitch rate, rad/sec
Pitch angle, rad
Normal acceleration, g
Actuator position, rad
Actuator position, rad
Actuator position, rad

The system matrix A, the control input matrix G_1, and measurement matrix M are

Matrix A

	1-Column	2-Column	3-Column	4-Column	5-Column	6-Column	7-Column	8-Column
1-Row	-0.4508E-01	-0.6762E+02	-0.7431E+02	-0.1054E+03	0.3032E+03	-0.1944E+03	0.9094E+01	-0.3556E+02
2-Row	.2142E-04	-.2498E+01	.9870E+00	-.7683E-03	-.1388E+02	-.7456E-01	.3703E+00	-.1362E+01
3-Row	-.6060E-3	.7241E+02	-.3803E+01	.1187E-02	-.3414E+04	-.1961E+04	.6843E+03	-.4722E+03
4-Row	0	0	.1000E+01	0	0	0	0	0
5-Row	0	0	0	0	-.4000E+02	0	0	0
6-Row	0	0	0	0	0	-.4000E+02	0	0
7-Row	0	0	0	0	0	0	-.4000E+02	0
8-Row	0	0	0	0	0	0	0	-.4000E+02

Matrix G

	1-Column	2-Column	3-Column	4-Column
1-Row	0	0	0	0
2-Row	0	0	0	0
3-Row	0	0	0	0
4-Row	0	0	0	0
5-Row	.1000E+01	0	0	0
6-Row	0	.1000E+01	0	0
7-Row	0	0	.1000E+01	0
8-Row	0	0	0	.1000E+01

Matrix M

	1-Column	2-Column	3-Column	4-Column	5-Column	6-Column	7-Column	8-Column
1-Row	0.3040E+00	0	0	0	0	0	0	0
2-Row	0	.1000E+01	0	0	0	0	0	0
3-Row	0	0	.1000E+01	0	0	0	0	0
4-Row	0	0	0	0.1000E+01	0	0	0	0
5-Row	.1969E-05	-.7533E+02	-.3930E+00	.1406E-03	-.4185E+03	-.2249E+03	.1117E+02	-.4108E+02
6-Row	0	0	0	0	0	.4000E+02	0	0
7-Row	0	0	0	0	0	0	.4000E+02	0
8-Row	0	0	0	0	0	0	0	.4000E+02

As stated previously, the control system is to be implemented with a digital computer. Two approaches to synthesizing the discrete control system to be used in the computer can be taken: discrete digital synthesis or the conversion of a continuous design. Although the design methodology has a direct analogy for the discrete equations and could be used to design a discrete controller, the conversion of a continuous design to a discrete controller was used for this report.

DESIGN RESPONSE SELECTION

The cost function used in this design was formulated from the rate of the implicit model following error response. If the rigid body (subscript RB) and the implicit model (subscript m) equations are given by

$$\dot{x}_{RB} = A_{RB}x_{RB} + Bu \tag{4}$$

$$\dot{x}_m = A_m x_m + Bu \tag{5}$$

then the rate of residual can be defined as

$$\dot{r}_1 = \frac{d}{dt}(x_{RB} - x_m) \tag{6}$$

and is given by

$$\dot{r}_1 = A_{RB}x_{RB} - A_m x_m \tag{7}$$

Assuming that the rigid body and model states are close together

$$x_m \approx x_{RB} \tag{8}$$

yields

$$\dot{r}_1 = (A_{RB} - A_m)x_{RB} \tag{9}$$

The implicit model was chosen so that the short-period response had a critical damping ratio of 0.707 and a natural frequency of 3 rad/sec. The implicit phugoid model retained the RPRV's natural frequency (0.15 rad/sec), but had an increased critical damping ratio of 0.7. These values can be compared with the open-loop pole locations in figure 1.

The objective is to find an implicit model of similar form except that the roots of the characteristic equation result in these performance specifications. Extracting the short-period approximation from equation (1) (that is, assuming the velocity constant) and dropping the θ equation yields

$$\begin{bmatrix} \dot{\alpha} \\ \dot{q} \end{bmatrix}_{RB} = \begin{bmatrix} -2.498 & 0.987 \\ 72.41 & -3.803 \end{bmatrix} \begin{bmatrix} \alpha \\ q \end{bmatrix}_{RB} \tag{10}$$

If the elements of the $\dot{\alpha}$ equation are assumed to be identical in both the model and vehicle, then the remaining terms of the model can be specified. This requires the solution of the following equation:

$$\begin{vmatrix} s + 2.498 & -0.987 \\ -A_1 & s - A_2 \end{vmatrix} = s^2 + 2(0.707)3s + 3^2 \tag{11}$$

Performing the required calculations for A_1 and A_2 results in the following short-period implicit model:

$$\begin{bmatrix} \dot{\alpha} \\ \dot{q} \end{bmatrix}_m = \begin{bmatrix} -2.498 & 0.987 \\ -4.703 & -1.745 \end{bmatrix} \begin{bmatrix} \alpha \\ q \end{bmatrix}_m \tag{12}$$

An identical procedure can be used to calculate the phugoid implicit model

$$\begin{bmatrix} \dot{v} \\ \theta \end{bmatrix}_m = \begin{bmatrix} -8.02 & -105.41 \\ 0 & 0 \end{bmatrix} \begin{bmatrix} v \\ \theta \end{bmatrix}_m \tag{13}$$

By using this implicit model for the short-period and phugoid motion and enforcing the kinematic constraint that the pitch angle θ is equal to the integral of the pitch rate q, it follows directly from equation (9) that the design responses are

$$\bar{r}_1 = \begin{bmatrix} 7.98 & 0.001 & -0.002 & 0.005 \\ 0 & 77.11 & -2.06 & 0 \end{bmatrix} \begin{bmatrix} v \\ \alpha \\ q \\ \theta \end{bmatrix} \tag{14}$$

DESIGN EXAMPLES

Several design models are presented and discussed to illustrate the different controller designs generated by each design model and to gain insight as to why the form of the final design model was chosen. The details of the methodology for the method used in this report are given in the appendix. The design process begins with the basic airplane as described by equations (2) and (3) augmented with the elevator being driven with filtered zero mean Gaussian noise. The elevator was chosen for the injection of the noise because it produced sufficient root mean square (rms) levels on all the states. Experience has shown that if the injected noise does not excite the system sufficiently, the incremental gradient procedure may not converge.

Basic Design Model

In the full-state feedback LQR solution, the characteristics of the noise process do not affect the resultant gains. However, in the reduced state feedback case, the calculated gains are dependent on these characteristics (that is, the eigenvalues of the shaping filter with respect to the eigenvalues of the open-loop system). Since the design objective of this controller is a stability augmentation system, it is only necessary to place the eigenvalues of the noise filter outside a circle which is centered at the origin and which encloses the eigenvalues of the open-loop systems that are important. An additional constraint in solving the Riccati equation (eq. (A9)) requires that the initial eigenvalues be stable; therefore, the location of the noise filter pole was chosen on the negative real axis at 50 radians. However, if the design objective were gust alleviation, the gust filter would be based on an approximation of atmospheric turbulence. The rms output of the noise was arbitrarily adjusted to 0.1 radian. The structure of the basic design model is illustrated in figure 2.

By using the design response as defined by equation (14) with the matrix R (eq. (A16)) equal to the identity matrix, full-state feedback gains were calculated for several values of ρ. These results are presented in figure 3. The asymptotic behavior of the roots approaching Butterworth patterns is illustrated as ρ approaches zero. For large values of ρ the cost function is equivalent to a cost function known as the "minimum pseudo-energy." It is characterized by reflecting all unstable eigenvalues about the imaginary axis while not disturbing the stable eigenvalue locations. For a value of ρ of 0.5×10^8, the unstable root at 0.5 radian has been rotated about the imaginary axis and the damping of the phugoid has been increased to a critical damping ratio of 0.7. The full-state feedback gains are presented in table II. Since stable eigenvalues on the real axis yield satisfactory handling qualities and since weighting the control tends to minimize the control rms required to stabilize the system, the minimum pseudo-energy was considered to be appropriate. Also, large ρ values are expected to result in smaller gain values.

An interesting observation can be made by noting that for this value of ρ, and in fact for any value of ρ, implicit model following is not achieved. Implicit model following is never obtained because the differences between the desired model and the plant are large enough to render equation (8) invalid. The fact to be noted is that although the design did not minimize the cost as it was anticipated, the control law produced was good.

By using this form of the weighting matrix and the design model as shown in figure 2, the incremented gradient procedure was applied. The output feedback gains are shown in table III and the closed-loop eigenvalues can be compared with the open-loop eigenvalues in figure 1. The unstable root at 5 radians has been rotated about the imaginary axis and the damping of the phugoid has been increased to a critical damping ratio of 0.7. The response of the closed-loop linear system with the basic gains to a negative 0.1-radian step in the elevator command is illustrated by the time history of the pitch rate and elevator position in figure 4(a).

The response of the system is that of a well-damped θ command system. This is the predicted result of the response of the linear equations of motion of an aircraft to a step in the elevator, pitch angle being feedback. This response may not be the one that is desired for the aircraft, but it is an acceptable response for a SAS. Control laws designed in a similar manner can be added to modify this controller design for other control tasks, such as pitch rate command. The pitch rate does not return to zero because the linear equations were used in the simulation.

Figure 4 represents the time history of the response of the RPRV to a negative step in the elevator command, with and without simulated noise being added to the sensors. The upper half of the figure represents the response of the vehicle to the step command with no noise added to the sensor measurements, whereas the lower half is the response of the vehicle with noise, modeled by first-order low-pass filters with the parameter of table I, added to the sensors. In the lower left quadrant, the response of the pitch rate and elevator position have been significantly changed by the addition of noise to each of the sensor measurements. Since the design model did not account for the noise on the measurement, the gains that were obtained do nothing to attenuate the noise; thus, the response of the aircraft is undesirable in a noisy environment.

Design Model for Noise

In order to overcome this undesirable response, or at least minimize the effect of the noise, the design model was augmented as shown in figure 5. To each of the output signals, filtered noise was added at an intensity level equal to the calculated rms output of the assumed first-order filter of the observed flight records. The resulting gains from the design process are given in table IV. Comparing these gains with those in table III indicated an overall reduction in magnitude, with some gains being reduced greater than others. In particular, the gain of the angle-of-attack sensor α_s has been reduced significantly. This was to be expected since the rms output of this sensor was the largest. The most surprising result was a sign change on the normal acceleration a_z gains. There is no logical explanation for this result. A plausible reason for this difference could be in the numerical accuracy of the gradient algorithm used in the design procedure. The eigenvalues of the closed-loop system can be compared with the basic design in figure 1. The major difference in the roots is the combining of the actuator root with a short-period root to form an oscillatory root with a critical damping ratio of 0.7 and a natural frequency of 30 rad/sec. This is not considered an unreasonable demand on the actuator since it is within the response of the open-loop actuator. The response of the pitch rate due to a step response in the elevator for this control design can be compared with the identical simulation with the gains of table II in figure 4. The major differences between the closed-loop system responses are (1) the apparent short-period critical damping ratio has been decreased to about 0.7, and (2) the amount of noise transmitted by the SAS has been reduced.

Digital Implementation

Implementing control laws with a digital computer requires some form of digital-to-analog conversion. The most widely used method is the zero-order hold (ZOH). The degrading effects of using a ZOH are illustrated by a frequency response analysis in figure 6. The general nature of the degrading effects of the ZOH is the added phase lag in the low frequency range. In this figure the gain and phase characteristics of a ZOH without and with discrete compensation are plotted against the frequency of the input signal ω divided by the frequency of the sampler.

Hartmann, Hauge, and Hendrick (ref. 6) have proposed using the phase lead compensator depicted in figure 6 to improve these undesirable characteristics of the ZOH. In order to minimize these characteristics, this digital compensator was implemented in the control design, and a time history analysis of the closed-loop system was performed. The time histories did not indicate any change with or without the compensator being in the loop. This can be attributed to good gain and phase margins that accompany full state LQR design that have carried over to the partial state design.

In order to illustrate the effects of the compensator, a frequency analysis was performed on the continuous closed-loop system and the discrete closed-loop system with and without the ZOH compensator in the loop. The difference between these systems is shown in figure 7. In figure 8, the frequency response of the pitch rate q due to the system being excited with the elevator can be compared for the system with the basic gains and the system with the gains that have been designed for noisy measurements. Figure 9 compares the closed-loop frequency response effect of using the discrete ZOH phase lead compensator.

This analysis indicated that the effects of the ZOH on the closed-loop system are compensated for with the Z-domain transfer functions in figure 6, although these effects are not very strong. It is worth noting that this compensator for the ZOH has one major disadvantage, a pole in the left half of the Z-plane which produces an oscillation with a period of twice the sampling rate on the output. In this particular use, the oscillation did not produce any undesirable effects, but that is not to say that it could be used satisfactorily in all cases.

Design Model for Delay

The design model can be modified to account for the 1-cycle delay introduced by the digital implementation by including a filter representing a Padé approximation on the output of each actuator. This design model is shown in figure 10 with first-order functions used to represent the delay. The design process was repeated with several different order Padé approximations until the introduction of a higher order delay model did not change the resulting gains from the previous design model. For this example, the first-order approximation shown in figure 10 was sufficient to design the control system. These gains are presented in table V. A frequency analysis of the closed-loop system including a 1-cycle delay with the gains in tables IV and V can be compared in figure 11. As in the previous example, the differences between the

two systems is not great, but these examples illustrate methods for including the effects of the digital delay in the design model. In doing so, the resulting controller can be made to compensate for this delay. In this example, the compensation resulted in a shift of the amplitude ratio curve to the left, or to put it another way, the system low frequency gain was increased.

CONCLUSIONS

This paper presented a realizable optimal control system design for an RPRV from modern control theory design methodologies. The design methods for including noisy measurements, discrete controllers with zero-order-hold computational delay errors, and for finding design responses to achieve implicit model following have been presented in a design example for a remotely piloted research vehicle. Some important conclusions and results of this study are

1. The results of modern control theory design can be used to obtain realizable controller designs.

2. The effects of undesirable effects (i.e., noisy measurements, etc.) can be accounted for in the design model.

3. The robustness of LQR designs, in this example, was carried over into the realizable design.

4. An acceptable system was obtained although model following was not achieved.

Langley Research Center
National Aeronautics and Space Administration
Hampton, VA 23665
March 17, 1980

APPENDIX

DESIGN METHODOLOGY

The theory and numerical techniques used in the design procedure are documented in references 7 to 9 and, therefore, will only be summarized here. Given the time invariant linear system

$$\dot{x} = Ax + G_1 u + G_2 \eta \tag{A1}$$

$$r_1 = Hx + Du \tag{A2}$$

$$r_2 = Mx \tag{A3}$$

where x is the system state vector (including rigid-body states, actuator and servo states, sensor states, model following states, and wind states), u is the control input vector, and η is a unit-intensity white noise vector. The design response vector r_1 is a vector of elements that have been chosen so that when the squares of the elements are minimized, the desired performance of the system is obtained. The states, or linear combinations of the states, of the system which can be measured and are to be used in the final control system design are the elements of the measurement response vector r_2. The design methodology has two stages. Initially, a stabilizing control law of the form

$$u = Kx \tag{A4}$$

is found which minimized the performance index

$$J = E(r_1' Q r_1) = tr[QR_1] \tag{A5}$$

where E is the statistical expectation and Q is a symmetric weighting matrix. The matrix R_1 is the asymptotic response covariance matrix, defined as

$$R_1 = E(r_1 r_1') = (H + DK)X(H + DK)' \tag{A6}$$

where X is the asymptotic state covariance matrix. The closed-loop asymptotic state covariance matrix is the solution to

$$(A + G_1 K)X + X(A + G_1 K)' + G_2 G_2' = 0 \tag{A7}$$

APPENDIX

The full-state feedback gain matrix K is found by appending this covariance equation to J by a Lagrange multiplier matrix P and solving for the optimal (K,P,X) set which minimizes the augmented cost function. The resulting optimal gains K are

$$K = -(D'QD)^{-1}[G_1'P + D'QH] \tag{A8}$$

The Lagrange multiplier matrix P is found by solving the matrix Riccati equation

$$\tilde{A}'P + P\tilde{A} - P\tilde{E}P + \tilde{Q} = 0 \tag{A9}$$

where

$$\tilde{A} = A - G_1[D'QD]^{-1}D'QH \tag{A10}$$

$$\tilde{E} = G_1[D'QD]^{-1}G_1' \tag{A11}$$

$$\tilde{Q} = H'QH - H'QD[D'QD]^{-1}D'QH \tag{A12}$$

Insight into how to choose the matrices H and D and weighting matrix Q can be obtained by examining the preceding problem with the constraint

$$D'QH = 0 \tag{A13}$$

Reformatting the problem by substituting equation (A8) into equation (A4) and substituting the resulting equation into equation (A5) results in

$$J - E(\bar{r}_1'\bar{r}_1 + u'Ru) \tag{A14}$$

where

$$\bar{r} = Q^{1/2}Hx \tag{A15}$$

$$R = D'QD \tag{A16}$$

When R is replaced by ρR, where ρ is a scalar design parameter, Harvey, Stein, and Doyle in reference 10 have shown that as ρ tends to zero, the poles of the closed-loop response matrix $A - G_1(R)^{-1}G_1'P$ approach either (a) the

closed-loop transmission zeros that have negative real parts or the left half-plane mirror images of the zeros in the right half-plane, or (b) they approach infinity in multiple Butterworth patterns with different growth rates. Partitioning the matrices H and D so that equation (A13) is valid allows the elements of the Q matrix to individually control the effect of either equation (A15) or the control functions defined by the D matrix on the design. Increasing the weight on a response function (or control function) results in the rms of that function relative to the rms of the other functions to be lowered. By using a set of response functions, the requirement of finding the proper weights on the states is transformed into finding a smaller set of weights on the response functions. These response functions may have conflicting effects on each other; decreasing one particular function may tend to increase the response of other functions. By adjusting the weights on these functions, the performance of the design can be adjusted until a compromise solution is obtained to the controller design.

This formulation of the LQR problem has three advantages:

(1) The problem of choosing the quadric weights is reduced to that of finding a smaller set of design responses. These design responses may be intuitive from the design objective.

(2) The weights on the controls R are chosen to regulate the relative control motion with respect to each control; that is, the allowable maximum for control u_1 may be different than the allowable maximum for control u_2.

(3) The scalar parameter ρ can be considered a gain adjustment. As ρ tends to zero, the elements of the gain matrix K increase.

The design cycle consists of forming a design response $\bar{r}_1$, selecting the relative control weights R, and solving equations (A8) and (A9) for several values of the scalar parameter ρ. This design cycle is repeated until the performance of the system meets the design goals.

Once the designer is satisfied with the closed-loop performance of the system, an "incremental gradient" procedure is used in the second stage of the design procedure to reduce the full-state feedback control system to a reduced state or realizable control system. The full-state gain matrix represents the starting point for the "incremental gradient" procedure and, therefore, need not be calculated with this procedure. The initial gains can be calculated with any procedure as long as equation (A5) is minimized and the control law is of the form of equation (A4).

In the incremental gradient procedure, the measurement gains are written as a function of a scalar parameter λ so that

$$u = K^*(\lambda)\, x \tag{A17}$$

where

$$K^*(\lambda) = K_1(\lambda)\, M + \lambda K_2 \tag{A18}$$

By assuming M has maximal rank $K^*(1)$ is defined as

$$K^*(1) = K_1(1)\, M + K_2 \tag{A19}$$

where $K_1(1)$ is defined as

$$K_1(1) = KM'(MM')^{-1} \tag{A20}$$

and K is the full-state feedback matrix from equation (A4) and

$$K_2 = K[I - M'(MM')^{-1}M] \tag{A21}$$

The procedure determines the gain for use in equation (A17) as $K^*(\lambda)$ which is obtained by gradually letting λ move from $\lambda = 1$ to $\lambda = 0$ while maintaining

$$\frac{\partial \bar{J}}{\partial K_1(\lambda)} \equiv 0 \tag{A22}$$

with $\bar{J}$ a quadratic performance index of the form (A5) using the control law of equation (A17). Explicit details can be found in reference 10.

REFERENCES

1. Kwakernaak, Huibert; and Sivan, Raphael: Linear Optimal Control Systems. John Wiley & Sons, Inc., c.1972.

2. Anderson, Brian D. O.; and Moore, John B.: Linear Optimal Control. Prentice-Hall, Inc., c.1971.

3. Kirk, Donald E.: Optimal Control Theory - An Introduction. Prentice-Hall, Inc., c.1970.

4. Konar, A. F.; Stone, C. R.; Mahesh, J. K.; and Hank, M.: Active Control Synthesis for Flexible Vehicles. Volume 1 - KONPACT Theoretical Description. AFFDL-TR-75-146, U.S. Air Force, June 1976. (Available from DTIC as AD B015 198L.)

5. Elliott, Jarrell R.: NASA's Advanced Control Law Program for the F-8 Digital Fly-by-Wire Aircraft. IEEE Trans. Autom. Control, vol. AC-22, no. 5, Oct. 1977, pp. 753-757.

6. Hartmann, Gary L; Hauge, James A.; and Hendrick, Russell C.: F-8C Digital CCV Flight Control Laws. NASA CR-2629, 1976.

7. Konar, A. Ferit: Development of Weapon Delivery Models and Analysis Programs. Volume I - System Modeling and Performance Optimization. AFFDL-TR-71-123, U.S. Air Force, Apr. 1972. (Available from DTIC as AD 751 505.)

8. Stein, Gunter; and Henke, Allen H.: A Design Procedure and Handling-Quality Criteria for Lateral-Directional Flight Control Systems. AFFDL-TR-70-152, U.S. Air Force, May 1971.

9. Kowalik, J.; and Osborne, M. R.: Methods for Unconstrained Optimization Problems. American Elsevier Pub. Co., Inc., 1968.

10. Harvey, C. A.; Stein, G.; and Doyle, J. C.: Optimal Linear Control (Characterization of Multi-Input Systems). ONR CR 215-238-2, U.S. Navy, Aug. 1977. (Available from DTIC as AD A043 771.)

TABLE I.- NOISE PARAMETERS

Sensor	τ, sec	Intensity	Root mean square
v_s	0.16	0.61 m/sec	1.08 m/sec
α_s	0.005	0.3^o	3.00^o
q_s	0.08	0.5 deg/sec	1.25 deg/sec
θ_s	0.16	0.3^o	0.35^o
a_z	0.008	0.06g	0.47g

TABLE II.- FULL-STATE FEEDBACK GAINS

	v_s, m/s	α_s, rad	θ_s, rad	q_s, rad	a_z, g	δ_{fi}, rad	δ_c, rad	δ_{fo}, rad	x_g, rad
$\delta_{e,c}$, rad	-0.0012	2.366	0.1130	0.0762	0.0195	-0.0072	0.0342	-0.0079	0.2039
$\delta_{fi,c}$, rad	-0.0007	1.356	0.0647	0.0435	0.0112	-0.0041	0.0196	-0.0045	0.1168
$\delta_{c,c}$, rad	0.0002	-0.4599	-0.0220	-0.0115	-0.0038	0.0014	-0.0067	0.0015	-0.0397
$\delta_{fo,c}$, rad	-0.0002	0.3238	0.0155	0.0105	0.0027	-0.0010	0.0049	-0.0011	0.0279

TABLE III.- BASIC GAINS

	v_s, m/sec	α_s, rad	θ_s, rad	q_s, rad/sec	a_z, g
$\delta_{e,c}$, rad	-0.0010	2.054	0.1060	0.0668	0.0160
$\delta_{fi,c}$, rad	-0.0006	1.777	0.0607	0.0382	0.0091
$\delta_{c,c}$, rad	0.0002	-0.3991	-0.0206	-0.0137	-0.0031
$\delta_{fo,c}$, rad	-0.0001	0.2810	0.0145	0.0093	0.0022

TABLE IV.- GAINS DESIGNED FOR NOISE

	v_s, m/sec	α_s, rad	θ_s, rad	q_s, rad/sec	a_z, g
$\delta_{e,c}$, rad	-0.0009	0.0936	0.1278	0.1440	-0.0038
$\delta_{fi,c}$, rad	-0.0005	0.0530	0.0733	0.0827	-0.0022
$\delta_{c,c}$, rad	0.0002	-0.0179	-0.0251	-0.0301	0.0007
$\delta_{fo,c}$, rad	-0.0001	0.0126	0.0175	0.0202	-0.0005

TABLE V.- GAINS DESIGNED FOR NOISE AND DELAY

	v_s, m/sec	α_s, rad	θ_s, rad	q_s, rad/sec	a_z, g
$\delta_{e,c}$, rad	-0.0006	0.0840	0.1071	0.0881	-0.0043
$\delta_{fi,c}$, rad	-0.0004	0.0475	0.0615	0.0507	-0.0025
$\delta_{c,c}$, rad	0.0001	-0.0157	-0.0212	-0.0194	0.0008
$\delta_{fo,c}$, rad	-0.0001	0.0113	0.0147	0.0125	-0.0006

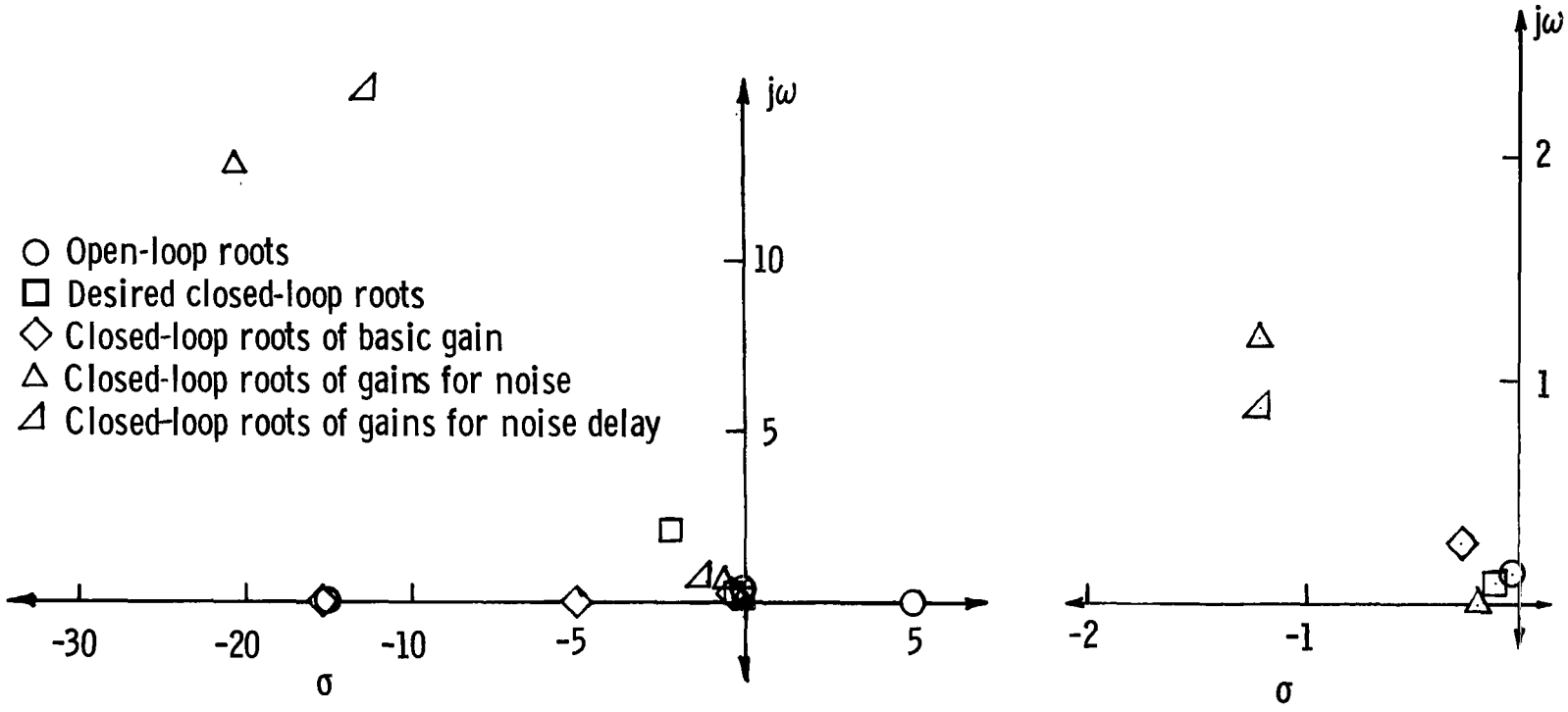

Figure 1.- Comparison of the roots of the characteristic equation for different design models. Note that high frequency roots are not shown.

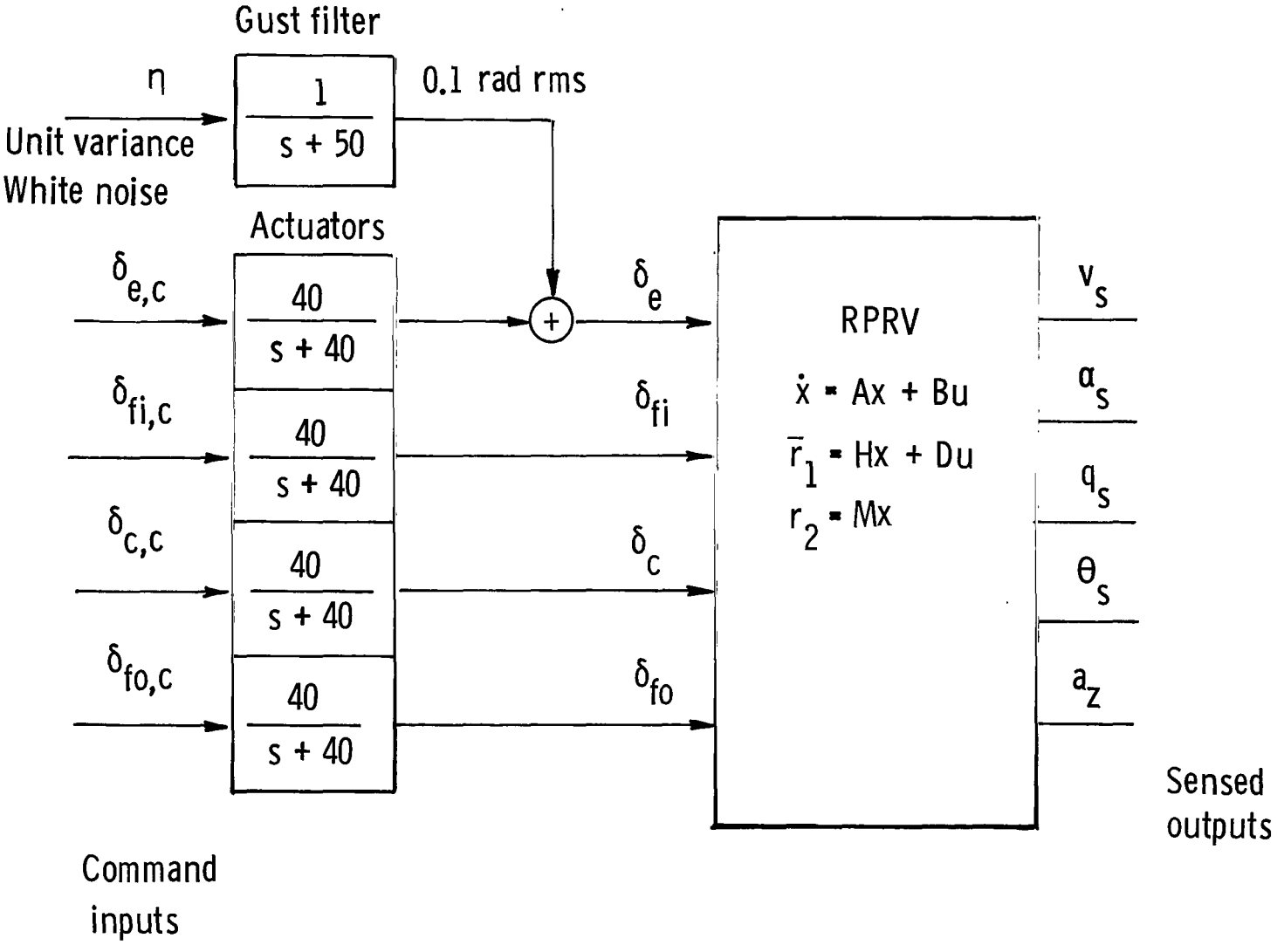

Figure 2.- Basic design model.

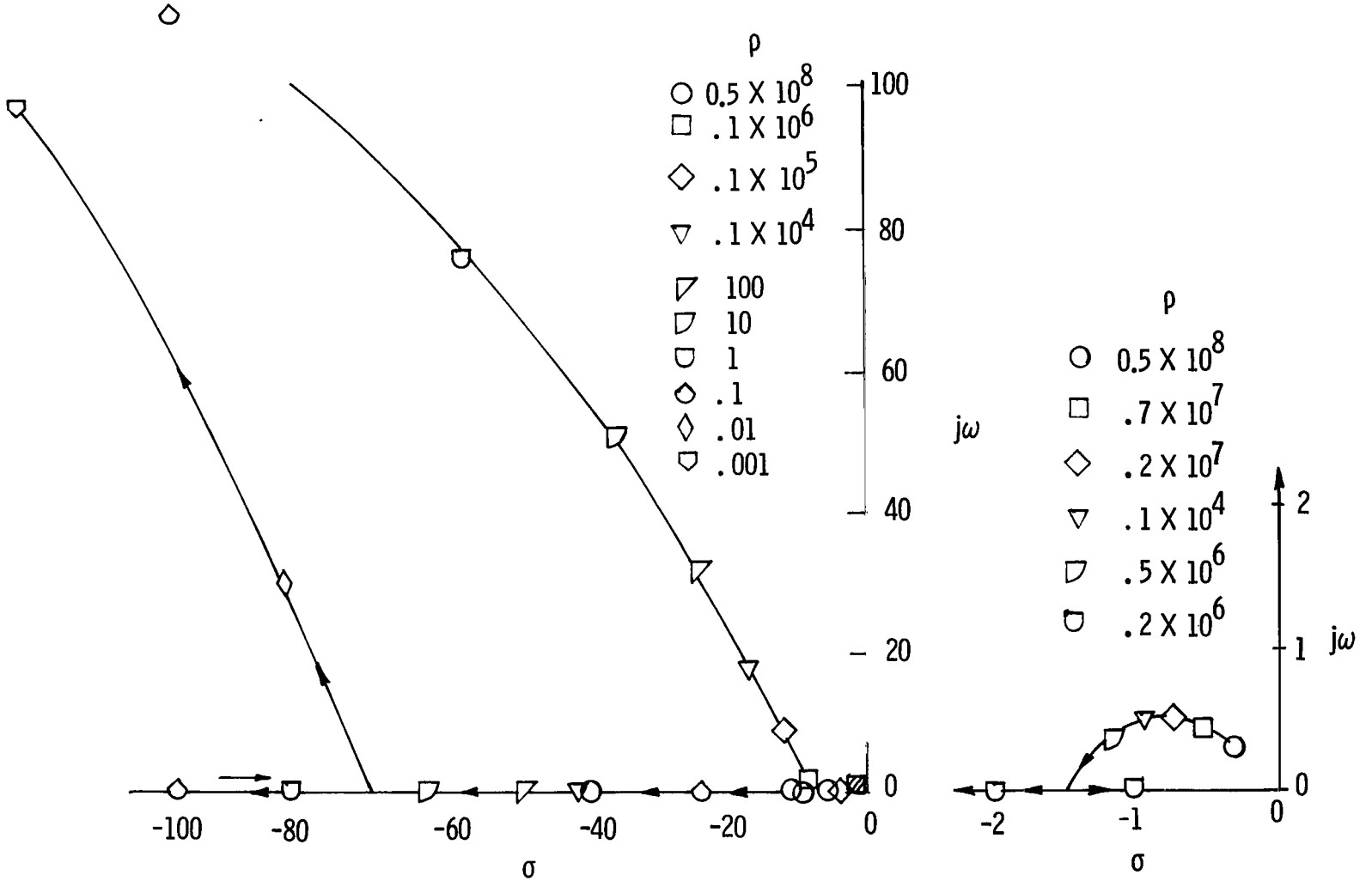

Figure 3.- Root locus of full-state feedback design varying design parameter ρ. Smaller plot is for cross-hatched area.

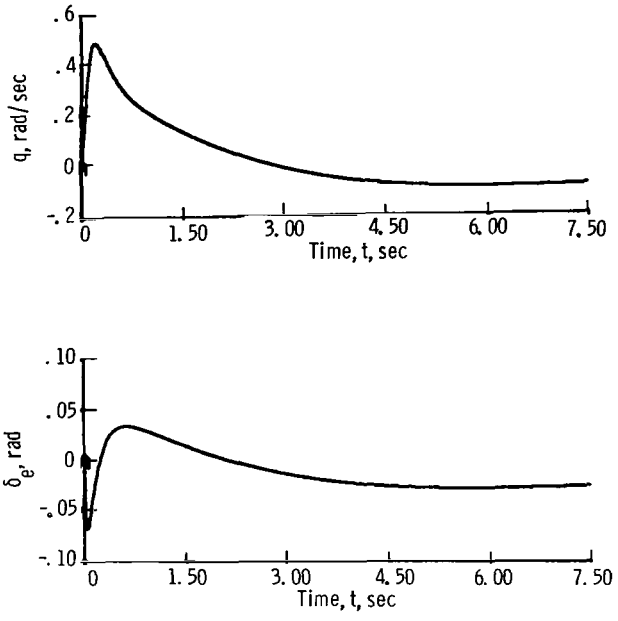

(a) Response with basic gains - no noise.

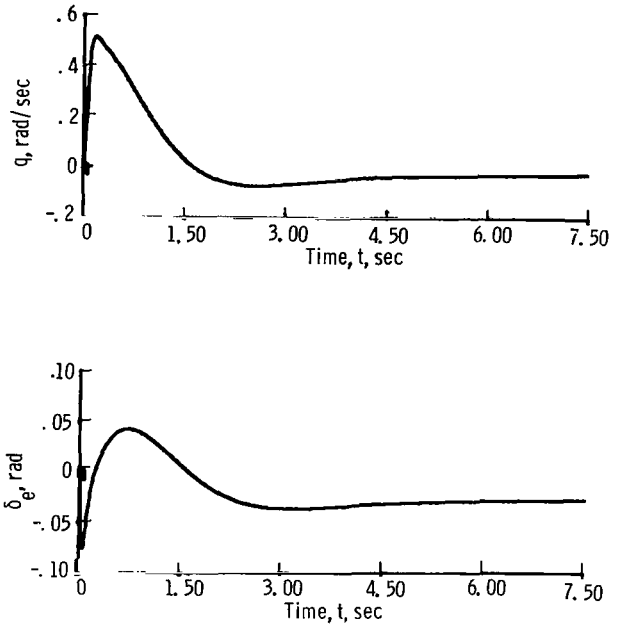

(c) Response with gains designed for noise - no noise.

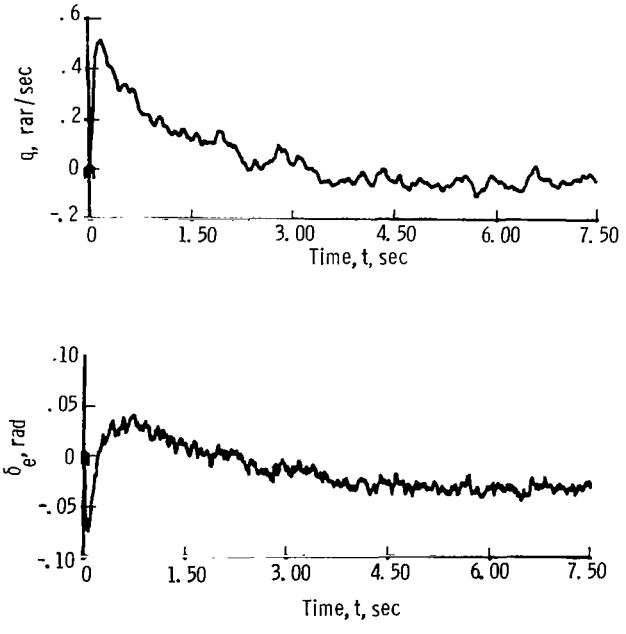

(b) Response with basic gains - noise on sensors.

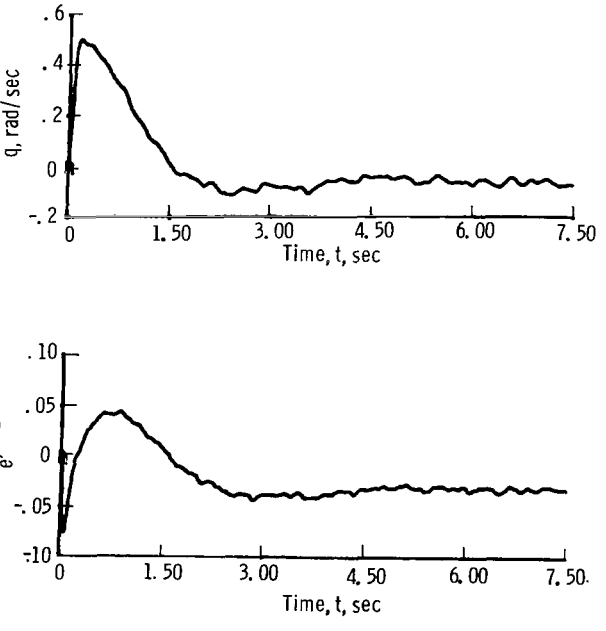

(d) Response with gains designed for noise - noise on sensors.

Figure 4.- Step response of pitch rate q and elevator position δ_e to a -0.1-radian step in elevator command for control design with and without sensor noise in the design model.

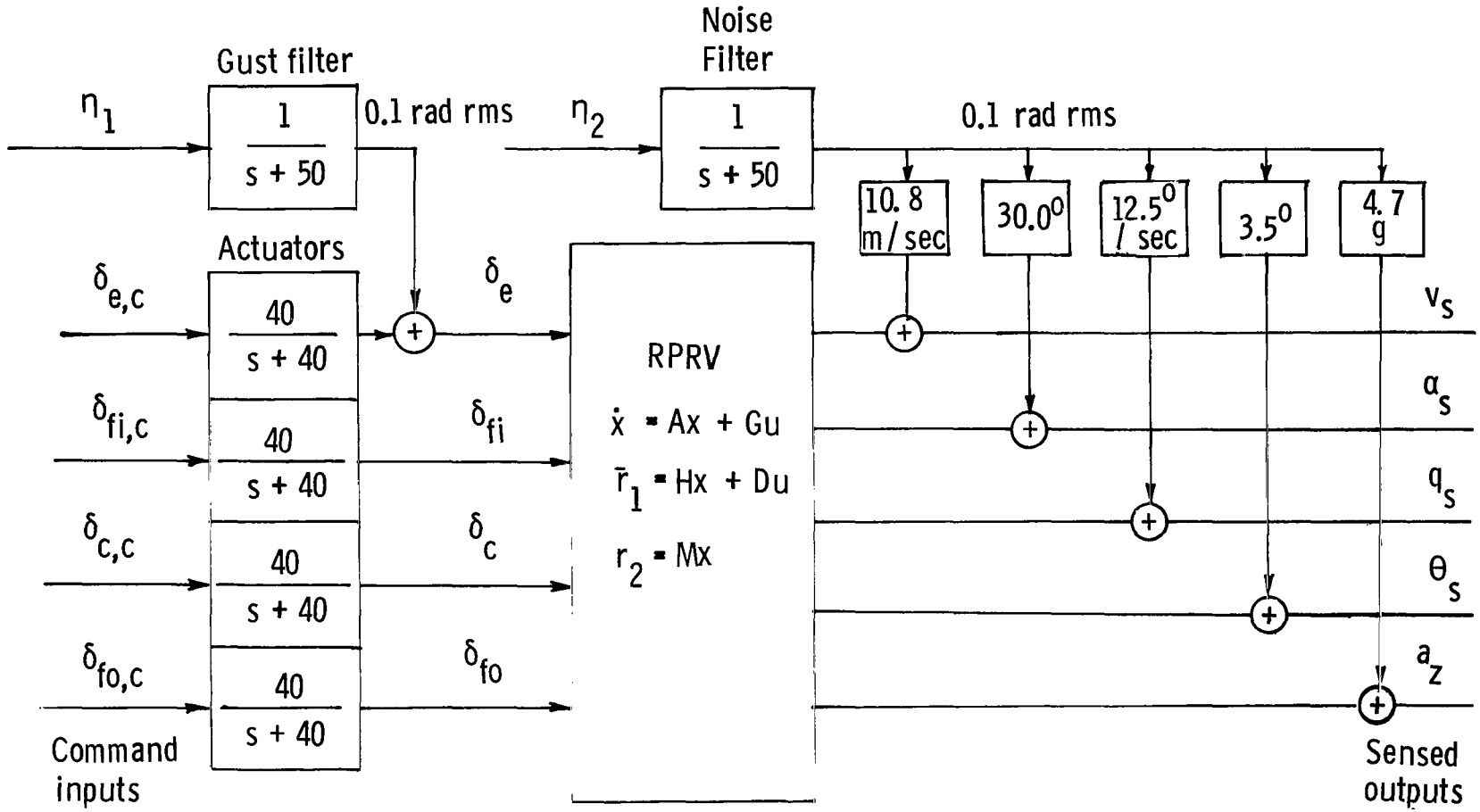

Figure 5.- Design model for noisy measurements.

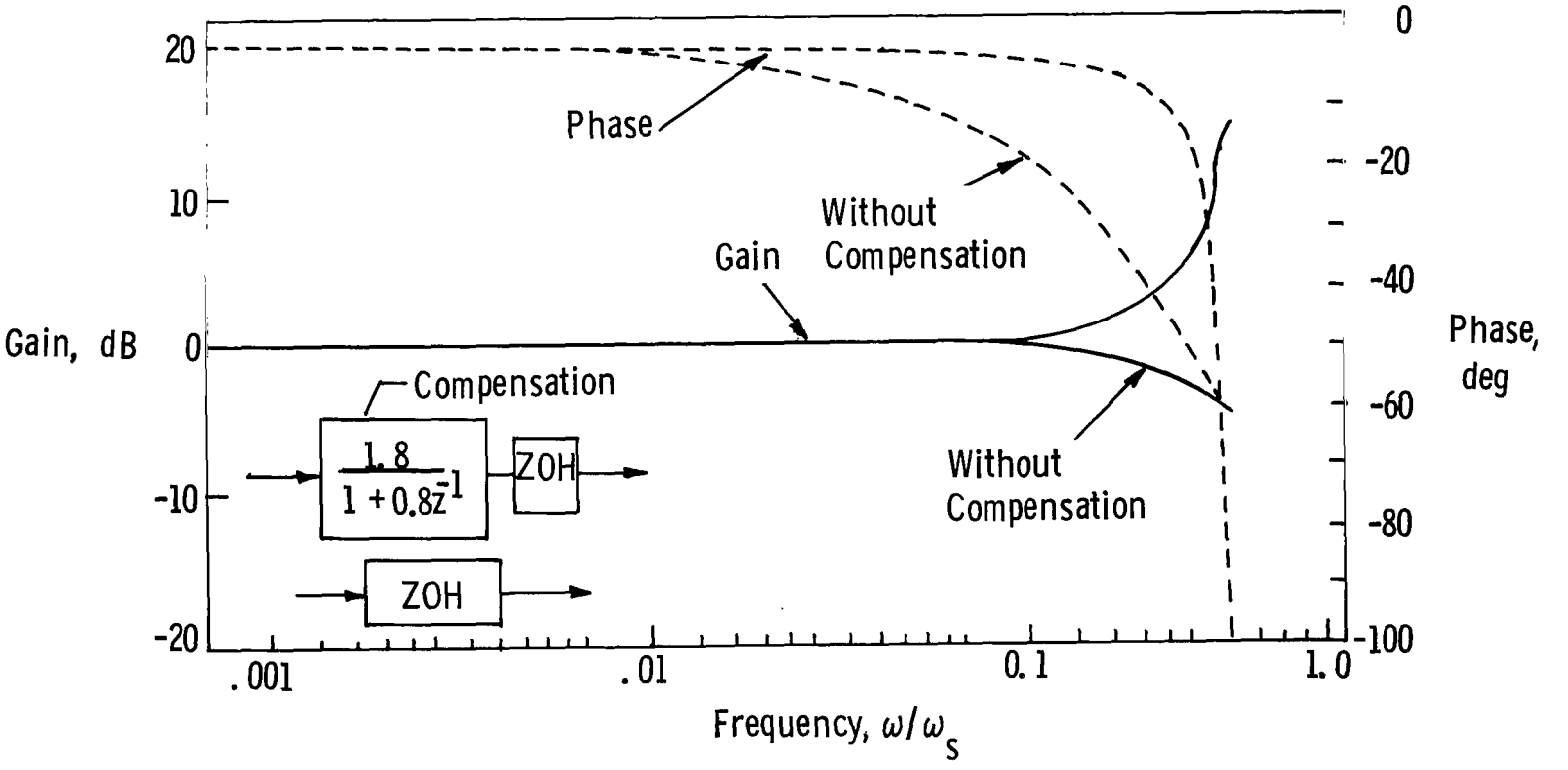

Figure 6.- Zero-order hold with and without phase lead compensation.

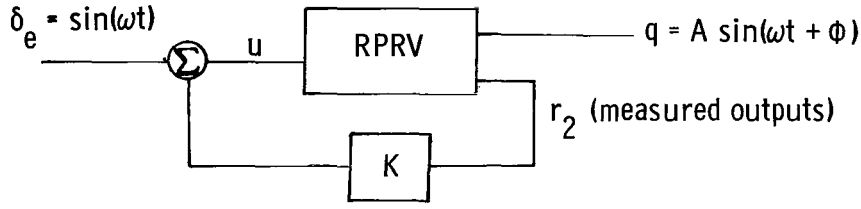

(a) Continuous closed-loop frequency response.

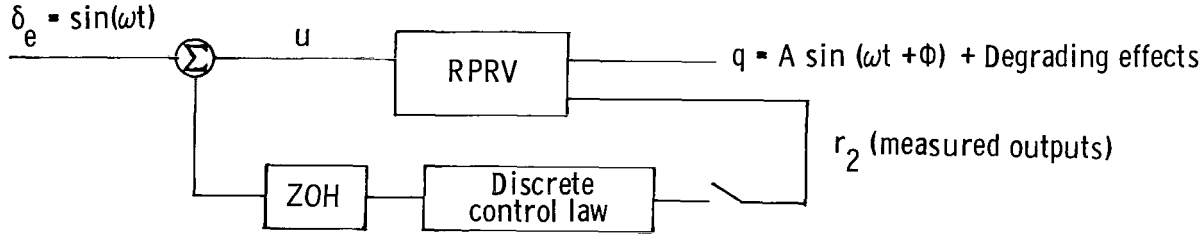

(b) Discrete closed-loop frequency response.

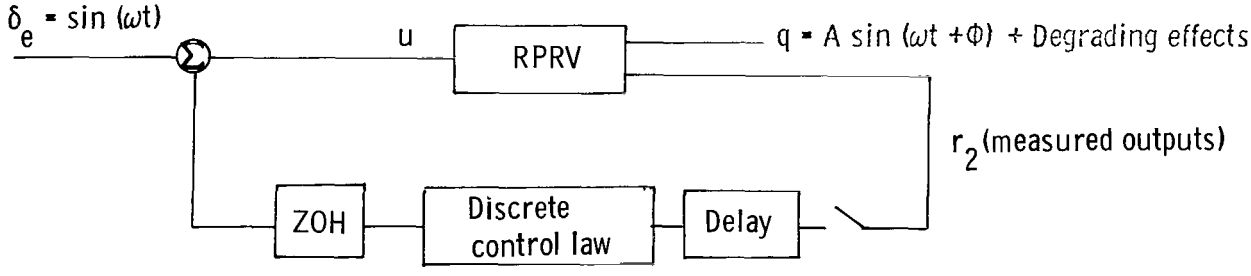

(c) Discrete closed-loop frequency response with delay.

Figure 7.- Frequency response models used to compare different control laws.

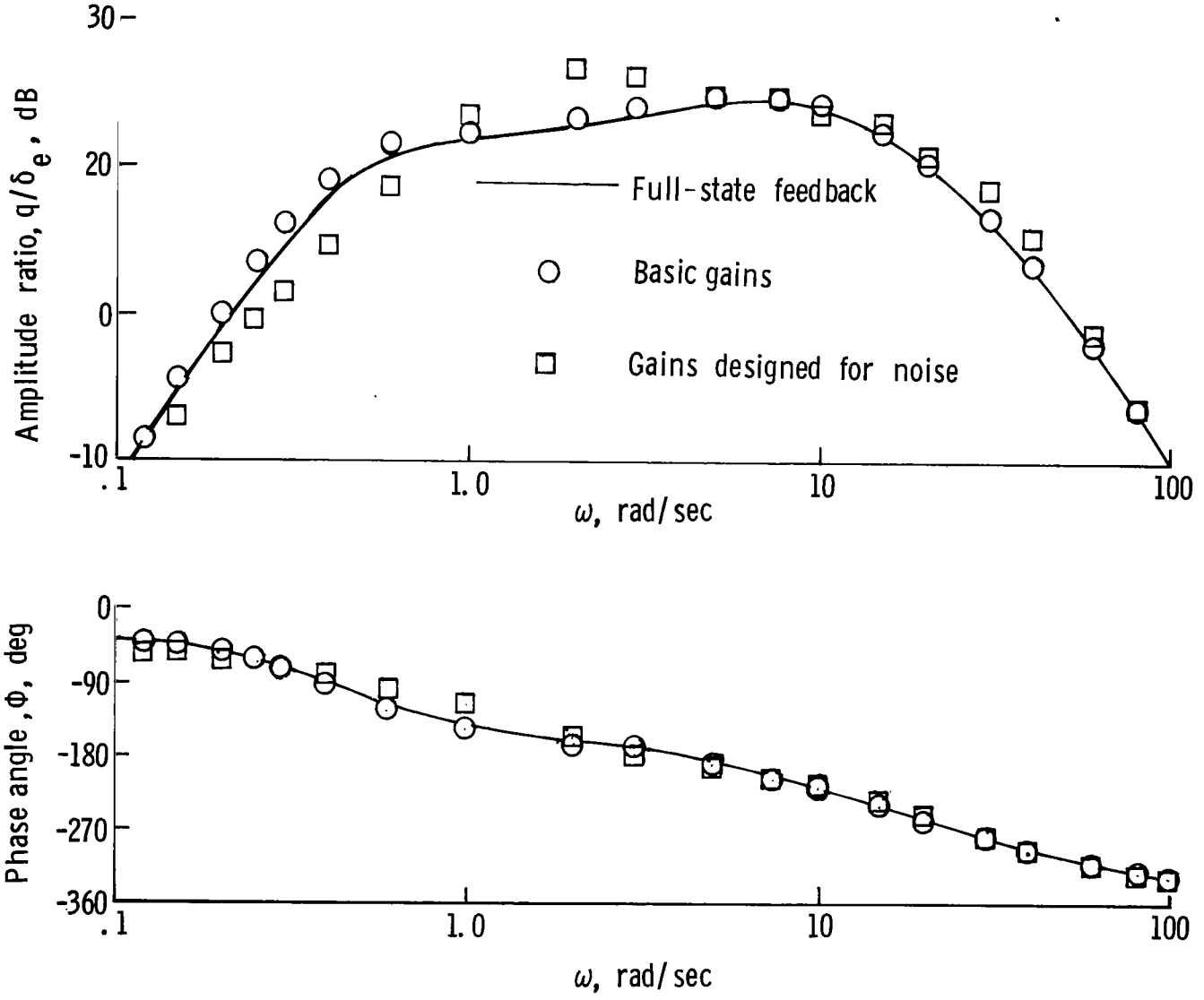

Figure 8.- Comparison of the full-state feedback, basic gains, and gains designed for noise.

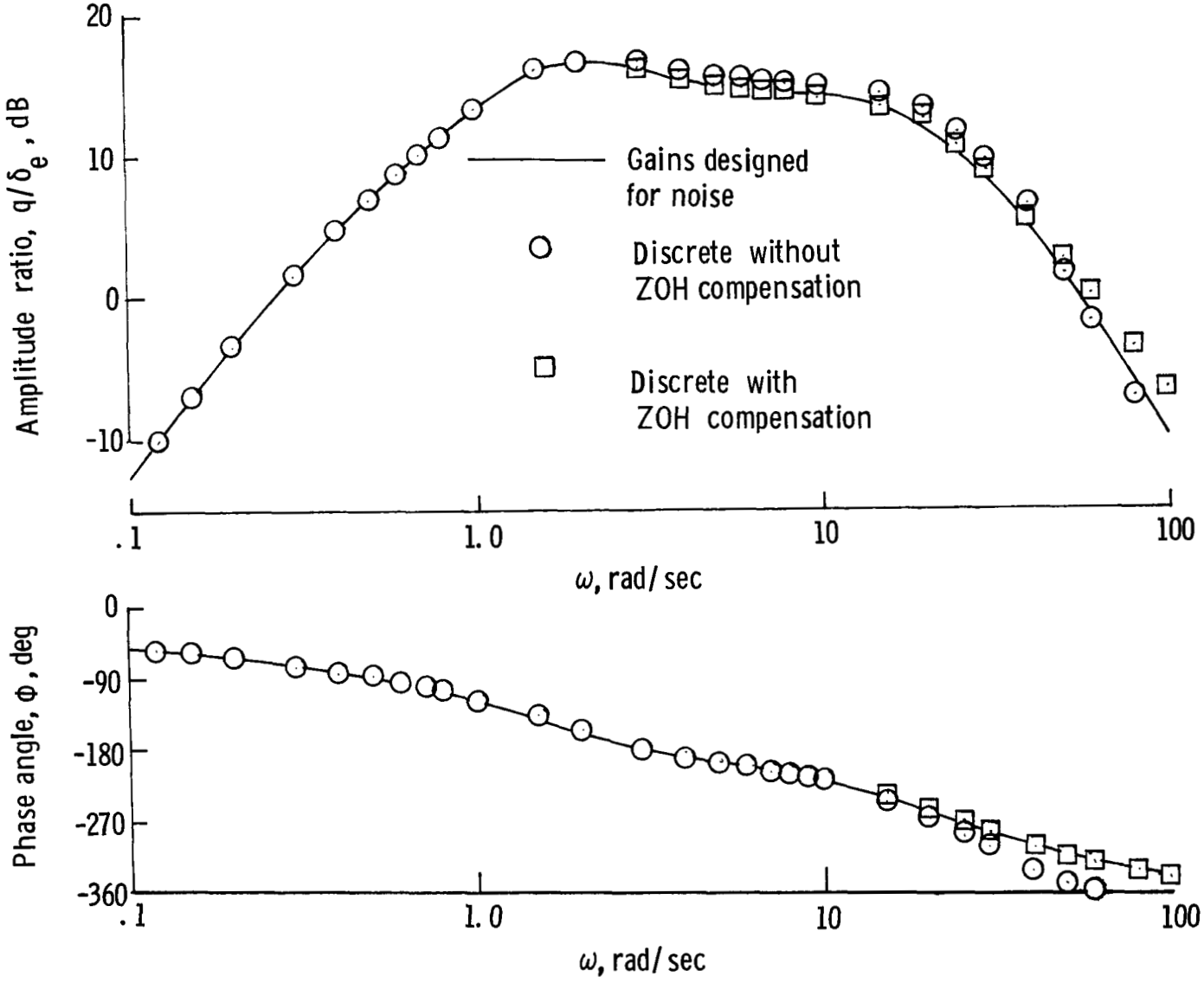

Figure 9.- Effect of the ZOH compensator on closed-loop response.

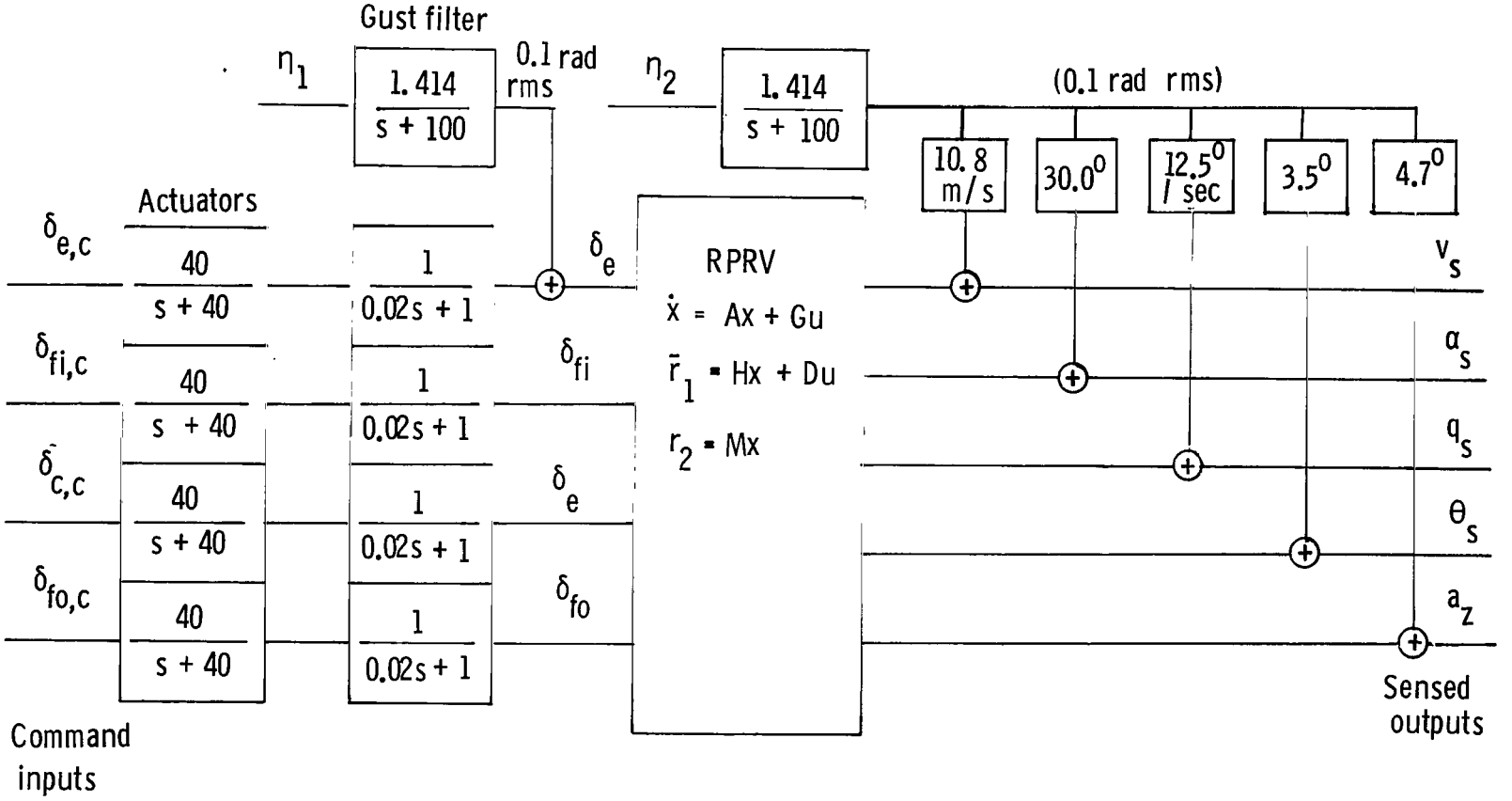

Figure 10.- Design model for noisy measurements with delay.

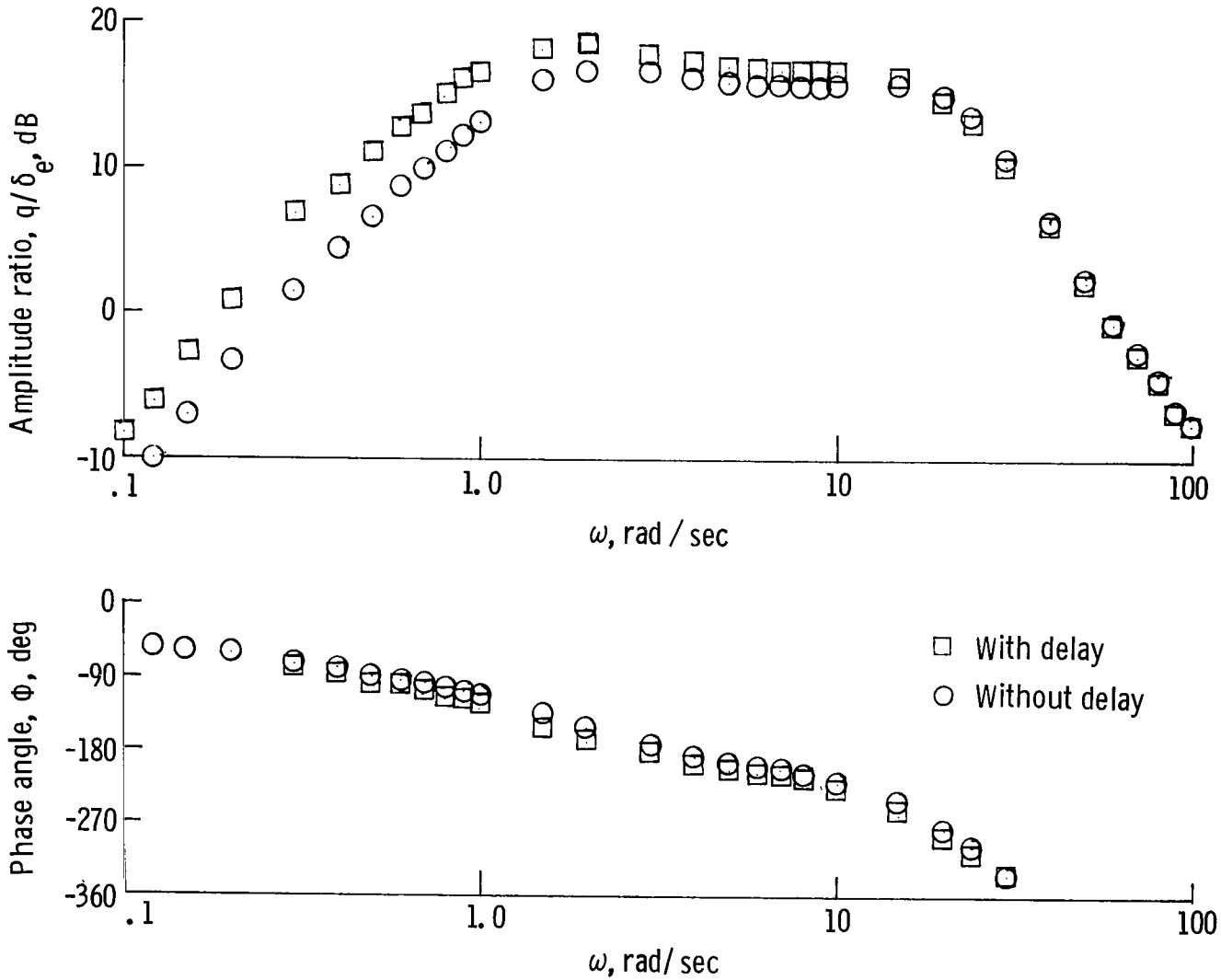

Figure 11.- Comparison of frequency response for design without delay model and for design with delay model.

1. Report No.	2. Government Accession No.	3. Recipient's Catalog No.
NASA TP-1654		

4. Title and Subtitle

REALIZABLE OPTIMAL CONTROL FOR A REMOTELY PILOTED RESEARCH VEHICLE

5. Report Date: May 1980

6. Performing Organization Code:

7. Author(s)

H. J. Dunn

8. Performing Organization Report No.: L-13403

10. Work Unit No.: 505-34-33-02

9. Performing Organization Name and Address

NASA Langley Research Center
Hampton, VA 23665

11. Contract or Grant No.:

13. Type of Report and Period Covered: Technical Paper

12. Sponsoring Agency Name and Address

National Aeronautics and Space Administration
Washington, DC 20546

14. Sponsoring Agency Code:

15. Supplementary Notes

16. Abstract

The design of a control system using the linear-quadratic regulator (LQR) control law theory for time invariant systems in conjunction with an "incremental gradient" procedure is presented. The incremental gradient technique reduces the full-state feedback controller design, generated by the LQR algorithm, to a realizable design. With a realizable controller, the feedback gains are based only on the available system outputs instead of being based on the full-state outputs. The design is for a remotely piloted research vehicle (RPRV) stability augmentation system. The design includes methods for accounting for noisy measurements, discrete controls with zero-order-hold outputs, and computational delay errors. Results from simulation studies of the response of the RPRV to a step in the elevator and frequency analysis techniques are included to illustrate these abnormalities and their influence on the controller design.

17. Key Words (Suggested by Author(s))	18. Distribution Statement
Optimal control theory Multi input/output Linear quadratic regulator	Unclassified - Unlimited Subject Category 63

19. Security Classif. (of this report)	20. Security Classif. (of this page)	21. No. of Pages	22. Price*
Unclassified	Unclassified	32	$4.50

For sale by the National Technical Information Service, Springfield, Virginia 22161

NASA-Langley, 1980

2 1 1U,G, 050580 S00903DS
DEPT OF THE AIR FORCE
AF WEAPONS LABORATORY
ATTN: TECHNICAL LIBRARY (SUL)
KIRTLAND AFB NM 87117